J Fluoresc (2011) 21:1599–1605
DOI 10.1007/s10895-011-0848-9

ORIGINAL PAPER

An NBD-based Sensitive and Selective Fluorescent Sensor for Copper(II) Ion

Shi-Rong Liu · Shu-Pao Wu

Received: 8 November 2010 / Accepted: 12 January 2011 / Published online: 28 January 2011

Abstract A new 7-nitrobenz-2-oxa-1,3-diazole (NBD) derived fluorescent probe (**1**) exhibiting high selectivity for Cu^{2+} detection, produced significant fluorescence quenching in the presence of Cu^{2+} ion, while the metal ions Ca^{2+}, Cd^{2+}, Co^{2+}, Fe^{2+}, Hg^{2+}, Mg^{2+}, Mn^{2+}, Ni^{2+} and Zn^{2+} produced only minor changes in fluorescence. The apparent association constant (K_a) for Cu^{2+} binding in chemosensor **1** was found to be 1.22×10^3 M^{-1}. The maximum fluorescence quenching activity caused by Cu^{2+} binding to **1** was observed over the pH range 6–10.

Keywords Cu(II) · Fluorescent chemosensor · NBD · *N*-(2-aminoethyl)picolinamide

Introduction

Ionic copper is the third most abundant essential transition metal ion in the human body, and plays important roles in various biological processes. Many proteins use copper ions as a cofactor for electron transport, O_2 transport, and catalysis of oxidation-reduction reactions [1]. Free copper ions in live cells catalyze the formation of reactive oxygen species (ROS) that can damage lipids, nucleic acids, and proteins. Research has connected the cellular toxicity of copper ions with serious diseases including prion disease [2], and Menkes and Wilson's disease [3, 4]. Due to its extensive applications, the copper ion is also a significant metal pollutant. The limit of copper in drinking water as set by the US Environmental Protection Agency (EPA) is 1.3 ppm (~20 μM). Several methods for the detection of copper ions have been proposed, including atomic absorption spectrometry [5], inductively coupled plasma mass spectroscopy (ICPMS) [6], and inductively coupled plasma-atomic emission spectrometry (ICP-AES) [7], and voltammetry [8]. These methods all provide good limits of detection (LOD) and wild concentration ranges. However, most of these methods require the use of costly apparatus and are not suitable for assays, because they involve destruction of the samples. Consequently, the development of fluorescent chemosensors for the detection of Cu^{2+} ions is attracting much research attention [9–23].

A general strategy used in developing metal ion chemosensors is to combine a metal-binding unit with signaling units such as chromophores or fluorophores. Changes in absorption wavelength or emission intensity during interaction with binding units, signals the presence of metal ions. The mechanism of Cu^{2+} recognition is a key issue for the design of Cu^{2+} chemosensors. Cu^{2+} can induce deprotonation of NH groups that are conjugated to aromatic compounds, or in amide bonds, upon Cu^{2+} binding. This deprotonation process caused by Cu^{2+} binding can be used for Cu^{2+} recognition. Peptides developed for copper ion sensing such as gly-his [10], gly-gly-his [9], and his-gly-gly-gly [18], can selectively bind Cu^{2+} to deprotonated amides.

In this study, we designed a 7-nitrobenz-2-oxa-1,3-diazole (NBD) based fluorescent chemosensor for metal ion detection. Two components make up chemosensor **1**; a NBD moiety as a reporter, and *N*-(2-aminoethyl)picolinamide as a metal ion chelator (Scheme 1). Binding metal ions to the chemosensor **1** causes fluorescence quenching of NBD. The metal ions Ca^{2+}, Cd^{2+}, Co^{2+}, Cu^{2+}, Fe^{2+}, Hg^{2+}, Mg^{2+}, Mn^{2+}, Ni^{2+} and Zn^{2+} were tested for metal ion binding selectivity with chemosensor **1**, and Cu^{2+} was the only ion that caused fluorescent quenching upon binding with chemosensor **1**.

S.-R. Liu · S.-P. Wu (✉)
Department of Applied Chemistry,
National Chiao Tung University,
Hsinchu, Taiwan 300, Republic of China
e-mail: spwu@mail.nctu.edu.tw

Scheme 1 Synthesis of chemosensor **1**

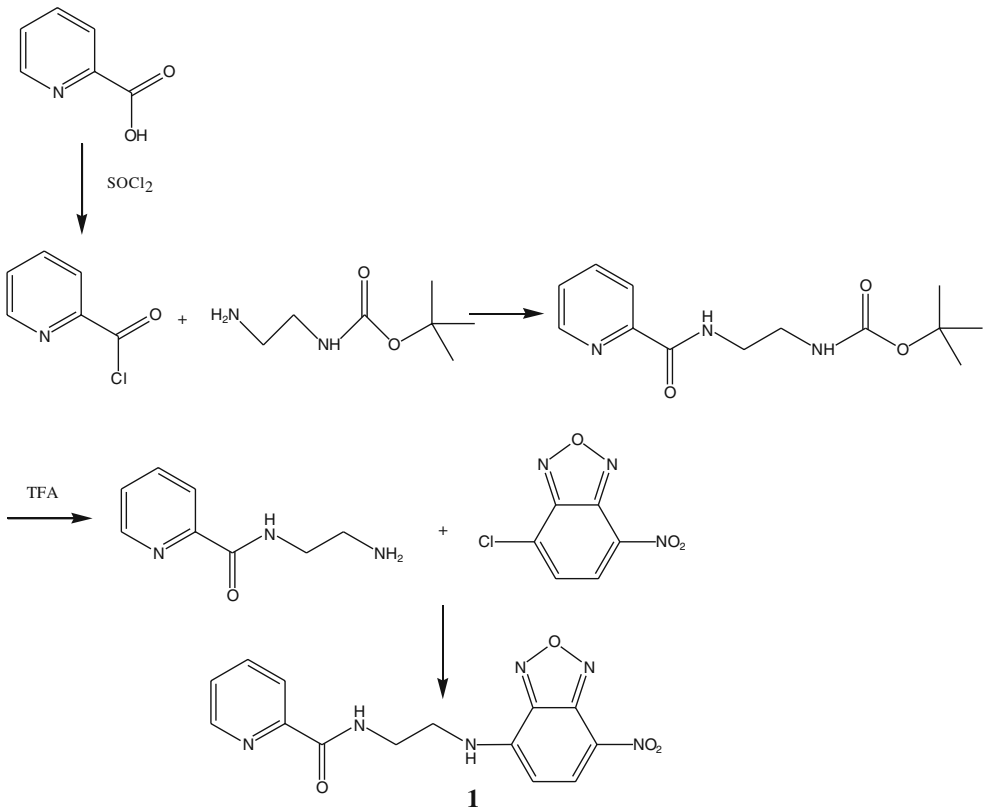

Experimental Section

Materials and Instrumentation

All solvents and reagents were obtained from commercial sources and used as received without further purification. UV/Vis spectra were recorded on an Agilent 8453 UV/Vis spectrometer. NMR spectra were obtained on a Bruker DRX-300 NMR spectrometer. IR data were obtained on Bomem DA8.3 Fourier-Transform Infrared Spectrometer.

Synthesis of *N*-(2-(picolinamido)ethyl)-7-nitrobenzo[c][1,2,5]oxadiazol-4-amine (chemosensors 1)

Que et al. reported a synthesis of *N*-(2-Aminoethyl)picolinamide by the reaction of ethyl picolinate with ethylenediamine [24]. In this study, we developed an alternative process to

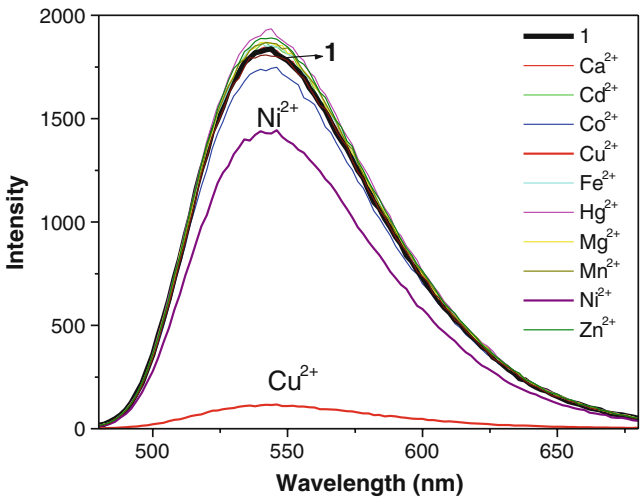

Fig. 1 Fluorescence response of chemosensor **1** (100 μM) to different metal ions (1 mM) in a methanol-water (*v*/*v*=1/1, 10 mM Hepes buffer, pH 7.0) solution. The excitation wavelength was 473 nm

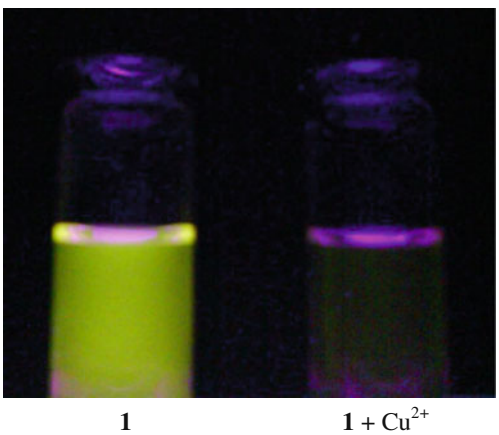

Fig. 2 Fluorescence of chemosensor **1** before and after quenching by the addition of Cu^{2+} in a methanol-water (*v*/*v*=1/1, 10 mM Hepes buffer, pH 7.0) solution

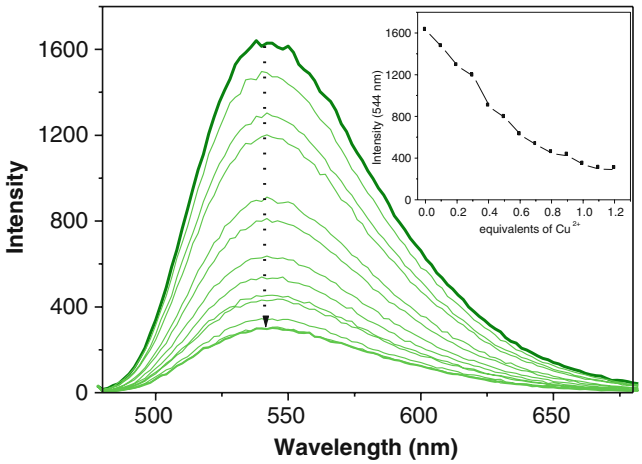

Fig. 3 Fluorescence response of chemosensor **1** (100 μM) with various Cu^{2+} ion concentrations, in a methanol-water (*v*/*v*=1/1, 10 mM Hepes buffer, pH 7.0) solution. The excitation wavelength was 473 nm

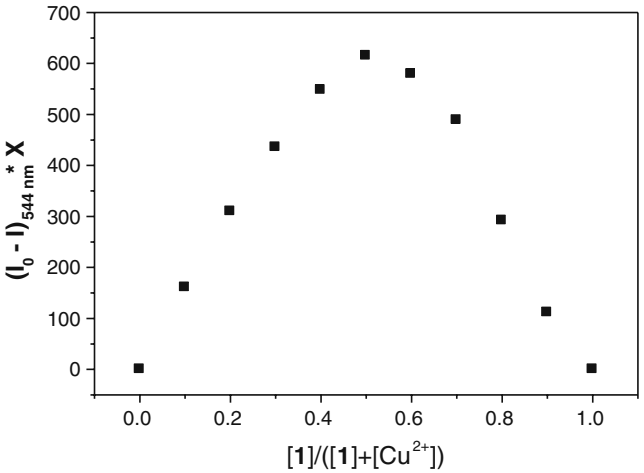

Fig. 5 Job plot of a 1:1 complex of **1**-Cu^{2+}, where the 544 nm emission is plotted against mole fraction of chemosensor **1**, at a constant total concentration of $2.0*10^{-4}$ M in a methanol-water (*v*/*v*= 1/1, 10 mM Hepes buffer, pH 7.0) solution

obtain *N*-(2-aminoethyl)picolinamide. A mixture containing picolinic acid (246 mg, 2.0 mmol) and thionyl chloride (146 μL, 2.0 mmol) in 30 mL CH_3CN was stirred for 5 min at 0°C. Triethylamine (420 μL, 3.0 mmol) and *tert*-butyl 2-aminoethylcarbamate (160 mg, 1.0 mmol) were added to the mixture and stirred for 12 h. The solvent was removed under reduced pressure, and the residue extracted with dichloromethane. The organic layer was dried over anhydrous $MgSO_4$. After evaporation of solvents, the product was obtained as a white solid. The white solid was dissolved in 15 mL CH_2Cl_2, and trifluoroacetic acid (1 mL) was added at 0°C. The mixture was allowed to warm to room temperature and stirred for 12 h. After evaporation, the product, *N*-(2-aminoethyl)picolinamide was obtained as brown oil in 93% yield, according to the amount of picolinic acid.

Further reaction of *N*-(2-aminoethyl)picolinamide (243 mg, 1.0 mmol) with NBD-Cl (245 mg, 1.2 mmol) was carried out with 15 mL of dichloromethane and triethylamine (169 μL, 1.2 mmol). The mixture was stirred at room temperature for 1 h. Thereafter, the solvent was evaporated under reduced pressure, and the crude product was purified by column chromatography (ethyl acetate: hexane = 1:1) to give **1** as a brown solid. Yield: 64%; mp: 225°C. MS (EI) *m*/*z* (rel intensity) 328 (M^+, 1%), 135 (91%), 123 (86%), 105 (100%), 78 (93%). HRMS *m*/*z* calcd for $C_{14}H_{12}N_6O_4$ $[M]^+$ 328.0920; *m*/*z* found 328.0913. ^{1}H NMR (300 MHz, DMSO-d_6) δ 9.54 (1H, brs, N*H*), 9.18 (1H, brs, N*H*), 8.65 (1H, d, *J*=4.0 Hz, Py*H*), 8.50 (1H, d, *J*=8.9 Hz, H_a), 8.05–.97(2H, m, Py*H*), 7.63–7.59 (1H, m, Py*H*), 6.53

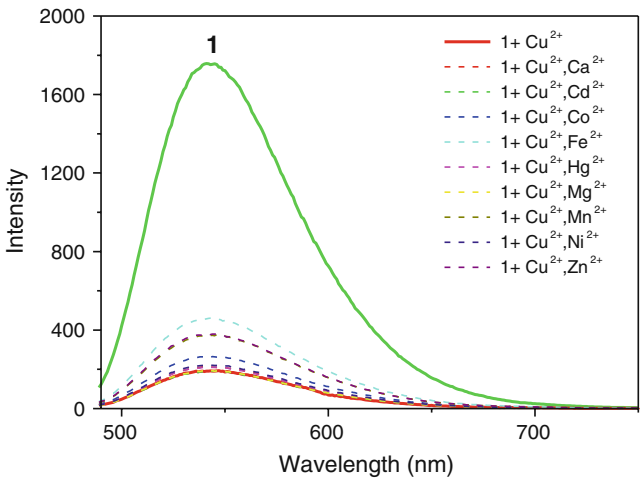

Fig. 4 Fluorescent response of **1** (100 μM) to Cu^{2+} (100 μM) over the selected metal ions (100 μM). All spectra were taken at 25°C in a methanol-water (*v*/*v*=1/1, 10 mM Hepes buffer, pH 7.0) solution at excitation wavelength 473 nm

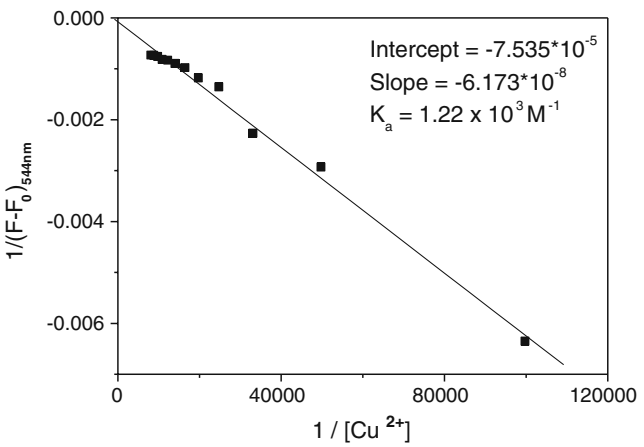

Fig. 6 Benesi-Hilderbrand plot of **1** with $Cu(BF_4)_2$

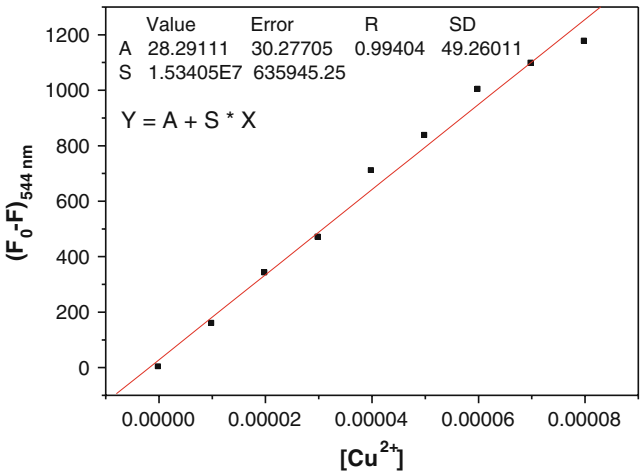

Fig. 7 Calibration curve of Cu^{2+}-**1** (100 μM) in a methanol-water (*v*/*v*= 1/1, 10 mM Hepes buffer, pH 7.0). The excitation wavelength was 473 nm, and the monitored emission wavelength was 544 nm. The detection limit (DL) of Cu^{2+} ions using chemosensor **1** was determined from the following equation: DL = K * SD/S, where K = 3; SD is the standard deviation of the blank solution; S is the slope of the calibration curve. DL = K * SD/S = 3 * 49.26011/1.53405*10^7 = 9.6*10^{-6} M (9.6 μM)

(1H, d, *J*=8.9 Hz, H_b), 3.67 (4H, s, CH_2); ^{13}C NMR (75 MHz, DMSO-d_6) δ 164.2, 149.6, 148.3, 145.2, 144.4, 137.7, 126.5, 121.8, 120.8, 99.3, 43.0, 37.1.

Metal Ion Binding Study by Fluorescence Spectroscopy

Chemosensor **1** (100 μM) was added with different metal ions (1 mM). All spectra were measured in 1.0 mL methanol-water solution (*v*/*v*=1/1, 10 mM Hepes buffer, pH 7.0). The light path length of cuvvet was 1.0 cm.

The pH Dependence on Cu^{2+} Binding in Chemosensor 1 Studied by Fluorescence Spectroscopy

Chemosensor **1** (100 μM) was added with Cu^{2+} (1 mM) in 1.0 mL methanol-water solution (*v*/*v*=1/1, 10 mM buffer). The buffers were: pH 1~2, KCl/HCl; pH 2.5~4, KH_2PO_4/HCl; pH 4.5~6, KH_2PO_4/NaOH; pH 6.5~10 Hepes.

Determination of the Binding Stochiometry and the Stability Constants K_a of Cu(II) Binding in Chemosensor 1

The binding stochiometry of **1**-Cu^{2+} complexes was determined by Job plot experiments [25]. The fluorescence intensity at 544 nm was plotted against molar fraction of **1** under a constant total concentration. The concentration of the complex approached a maximum absorbance when the molar fraction was 0.5. These results indicate that both chemosensor **1** forms a 1:1 complex with Cu^{2+}. The stability constants K_a of a 1:1 **1**-Cu^{2+} complexes were determined by the Benesi-Hilderbrand equation [26, 27]:

$$1/(F-F_0) = 1/\{K_a*(F_{max}-F_0)*[Cu^{2+}]\} + 1/(F_{max}-F_0) \quad (1)$$

, where F is the fluorescence intensity at 544 nm at any given Cu^{2+} concentration, F_0 is the fluorescence intensity at 544 nm in the absence of Cu^{2+}, and F_{max} is the maxima fluorescence intensity at 544 nm in the presence of Cu^{2+} in solution. The association constant K_a was evaluated graphically by plotting $1/(F–F_0)$ against $1/[Cu^{2+}]$. Typical plots ($1/(F–F_0)$ vs. $1/[Cu^{2+}]$) are shown in Fig. 6. Data were linearly fitted according to Eq. 1 and the K_a value was obtained from the slope and intercept of the line.

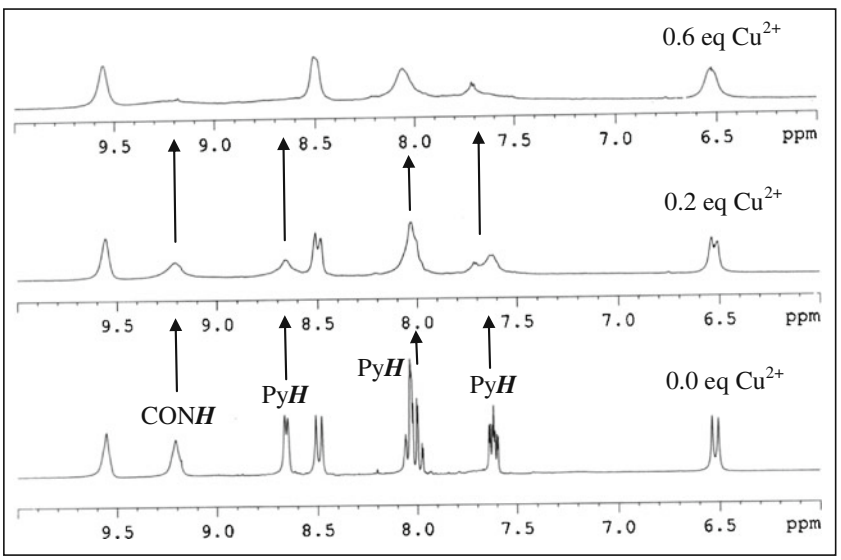

Fig. 8 ^1H NMR spectra of chemosensor **1** (5 mM) in the presence of different amount of Cu^{2+} in DMSO-d_6

Results and Discussion

Synthesis

Chemosensor **1** comprises two parts: an NBD moiety and *N*-(2-aminoethyl)picolinamide. Reaction of picolinoyl chloride with *tert*-butyl 2-aminoethylcarbamate in equimolar quantities, and deprotection with trifluoroacetic acid (TFA), furnished the chelator *N*-(2-aminoethyl)-picolinamide. The reaction of *N*-(2-aminoethyl)picolinamide with NBD-Cl provided Chemosensor **1** (Scheme 1). Chemosensor **1** is yellow, with an absorption band centered at 472 nm, and the sensor exhibits a green emission band centered on 544 nm with quantum yield, Φ=0.03.

Cation-sensing Properties

We tested the sensing ability of chemosensor **1** by mixing it with the metal ions Ca^{2+}, Cd^{2+}, Co^{2+}, Cu^{2+}, Fe^{2+}, Hg^{2+}, Mg^{2+}, Mn^{2+}, Ni^{2+} and Zn^{2+}. Figure 1 shows that addition of most metal ions did not cause a change in intensity; Cu^{2+} was the only ion that caused significant fluorescent quenching in chemosensor **1**. Upon binding with Cu^{2+}, the sensors green emission was completely quenched (Fig. 2). During Cu^{2+} titration with chemosensor **1**, the intensity of the 544 m emission band decreased (Fig. 3). After addition of greater than one molar equivalent of Cu^{2+}, the emission intensity reached a minimum. These observations suggest that Cu^{2+} is the only metal ion that readily binds with chemosensor **1**, causing significant fluorescence quenching, and permitting highly selective detection of Cu^{2+}.

To study the influence of other metal ions on Cu^{2+} binding with chemosensor **1**, we performed competitive experiments with other metal ions (100 μM) in the presence of Cu^{2+} (100 μM) (Fig. 4). Fluorescence quenching caused by the Cu^{2+} solution with most metal ions was similar to that caused by Cu^{2+} alone. This indicated that the other metal ions did not interfere significantly with the binding of chemosensor **1** with Cu^{2+}.

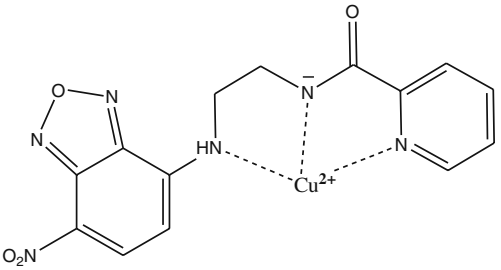

Fig. 10 A proposed 1:1 complex formed between **1** and Cu^{2+}

In order to understand the binding stoichiometry of chemosensor **1**-Cu^{2+} complexes, we carried out a series of Job plot experiments. Figure 5 plots the emission intensity at 544 nm against chemosensor **1** molar fraction, under a constant total concentration of **1**. Maximum fluorescent quenching occurred for a 0.5 mole fraction. This result indicates a 1:1 ratio for **1**-Cu^{2+} complexes, in which one Cu^{2+} ion binds with one chemosensor **1**. Evaluating the association constant, K_a, graphically by plotting $1/\Delta F$ against $1/[Cu^{2+}]$ produces Fig. 6. Linearly fitting the data to the Benesi–Hilderbrand equation, allows K_a to be determined from the slope and intercept of the plot. The apparent association constant, K_a, for Cu^{2+} binding in chemosensor **1** was determined as 1.22×10^3 M^{-1}. The detection limit of chemosensor **1** as a fluorescent sensor for the analysis of Cu^{2+} was determined from the plot of

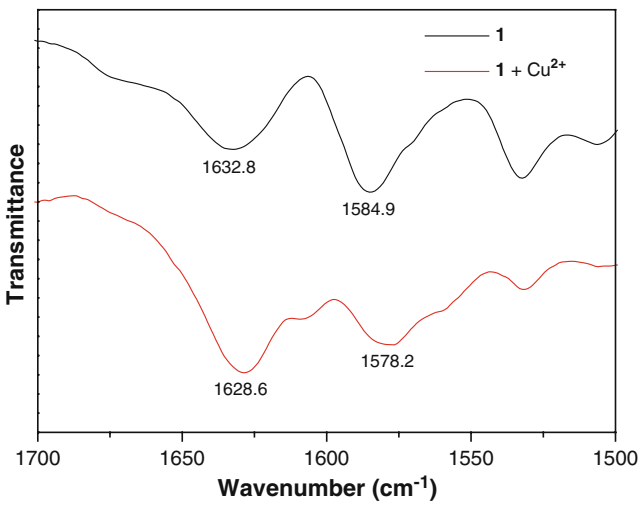

Fig. 9 IR spectra of chemosensor **1** in the presence of Cu^{2+} in methanol

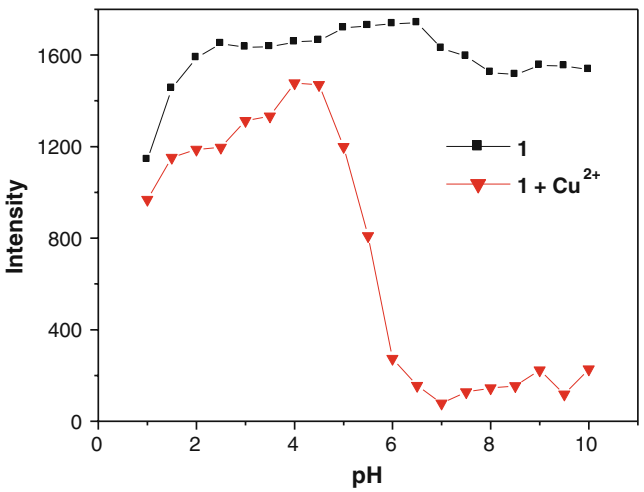

Fig. 11 Influence of pH on the fluorescence spectra for **1** (100 μM) both when pure, and in combination with Cu^{2+} (100 μM). The excitation wavelength was 473 nm, and the monitored emission wavelength was 544 nm

fluorescence intensity as a function of the concentration of Cu^{2+} (Fig. 7). It was found that chemosensor **1** has a detection limit of 9.6 μM, which is allowed for the detection of micromolar concentration range of Cu^{2+}.

To gain a clearer understanding of the structure of **1**-Cu^{2+} complexes, ^1H NMR and Infrared (IR) spectroscopy were employed. Cu^{2+} is a paramagnetic ion and can affect the proton signals that are close to Cu^{2+} binding site. In the ^1H NMR spectra of chemosensor **1** (Fig. 8), adding Cu^{2+} caused the proton (amide NH) signal at 9.2 ppm and the proton (at pyridine) signals at 7.6, 8.0, 8.65 ppm to almost completely disappear. Other peaks (protons at NBD) at 6.5, 8.5 ppm became broad upon Cu^{2+} addition. These observations indicated the binding of Cu^{2+} with an amide group, pyridine and an amine attached to the NBD motif. The IR spectra were primarily characterized by bands in the double-bond region (Fig. 9). The band 1,633 cm^{-1} was associated with double-bond (C=O) absorption in chemosensor **1**. Binding of Cu^{2+} with chemosensor **1** resulted in a shift from 1,633 cm^{-1} to 1,629 cm^{-1} in the double-bond absorption region, due to the amide group in chemosensor **1**. The Job plot indicates that the binding ratio for chemosensor **1**-Cu^{2+} complexes was 1:1. Cu^{2+} was bound to one nitrogen atom from pyridine, one nitrogen atom from amide and one nitrogen atom attached to the NBD motif (Fig. 10).

We performed pH titration of chemosensor **1** to investigate a suitable pH range for Cu^{2+} sensing. As depicted in Fig. 11, the emission intensities of metal-free chemosensor **1** remained unchanged. Only when pH was less than 3, did intensity slightly decreased. This was due to protonation of the bridging amine nitrogen, which bonds to NBD. In the presence of Cu^{2+}, the emission intensity at 544 nm suddenly decreased at pH 5.0 and reached lowest intensity in the range of pH 6 to pH 10. This indicates the formation of the **1**-Cu^{2+} complex at high pH values. This observation also reveals that the formation of the **1**-Cu^{2+} complexes is a deprotonation process (Fig. 10). Cu^{2+} binding induced protonation of the amide in chemosensor **1**. For pH < 5, the emission intensity remained higher due to the protonation of the amine groups, preventing the formation of **1**-Cu^{2+} complexes.

Conclusion

In conclusion, this study developed an NBD-based fluorescent chemosensor for Cu^{2+} ion sensing. We synthesized chemosensor **1** from the reaction of *N*-(2-aminoethyl)picolinamide and NBD-Cl, to form a new C–N bond between the two precursors. We observed significant fluorescence quenching with chemosensor **1** in the presence of Cu^{2+} ion, while, adding Ca^{2+}, Cd^{2+}, Co^{2+}, Fe^{2+}, Hg^{2+}, Mg^{2+}, Mn^{2+}, Ni^{2+}, or Zn^{2+} to the chemosensor solution caused only minimal changes in fluorescence emission intensity. The optimal pH range for Cu^{2+} detection by chemosensor **1** was pH 6–10. This NBD-based Cu^{2+} chemosensor provides an effective, and non-destructive means of Cu^{2+} ion sensing.

Acknowledgements We gratefully acknowledge the financial supports of the National Science Council (ROC) and National Chiao Tung University.

References

1. Cowan JA (1997) Inorganic biochemistry: an introduction. Wiley-VCH, New York, pp 133–134
2. Barnham KJ, Masters CL, Bush AI (2004) Neurodegenerative diseases and oxidative stress. Nat Rev Drug Discovery 3:205–214
3. Waggoner DJ, Bartnikas TB, Gitlin JD (1999) The role of copper in neurodegenerative disease. Neurobiol Dis 6:221–230
4. Vulpe C, Levinson B, Whitney S, Packman S, Gitschier J (1993) Isolation of a candidate gene for Menkes disease and evidence that it encodes a copper-transporting ATPase. Nat Genet 3:7–13
5. Gonzales APS, Firmino MA, Nomura C, Rocha FRP, Oliveira PV, Gaubeur I (2009) Peat as a natural solid-phase for copper preconcentration and determination in a multicommuted flow system coupled to flame atomic absorption spectrometry. Anal Chim Acta 636:198–204
6. Becker JS, Matusch A, Depboylu C, Dobrowolska J, Zoriy MV (2007) Quantitative imaging of selenium, copper, and zinc in thin sections of biological tissues (Slugs-Genus Arion) measured by laser ablation inductively coupled plasma mass spectrometry. Anal Chem 79:6074–6080
7. Liu Y, Liang P, Guo L (2005) Nanometer titanium dioxide immobilized on silica gel as sorbent for preconcentration of metal ions prior to their determination by inductively coupled plasma atomic emission spectrometry. Talanta 68:25–30
8. Ensafi AA, Khayamian T, Benvidi A (2006) Simultaneous determination of copper, lead and cadmium by cathodic adsorptive stripping voltammetry using artificial neural network. Anal Chim Acta 561:225–232
9. Torrado A, Walkup GK, Imperiali B (1998) Exploiting polypeptide motifs for the design of selective Cu(II) ion chemosensors. J Am Chem Soc 120:609–610
10. Zheng Y, Huo Q, Kele P, Andreopoulos FM, Pham SM, Leblanc RM (2001) A new fluorescent chemosensor for copper ions based on tripeptide glycyl−histidyl−lysine (GHK). Org Lett 3:3277–3280
11. Zeng L, Miller EW, Pralle A, Isacoff EY, Chang CJ (2006) A selective turn-on fluorescent sensor for imaging copper in living cells. J Am Chem Soc 128:10–11
12. Qi X, Jun EJ, Xu L, Kim S, Hong JSJ, Yoon YJ, Yoon J (2006) New BODIPY derivatives as off-on fluorescent chemosensor and fluorescent chemodosimeter for Cu^{2+}: cooperative selectivity enhancement toward Cu^{2+}. J Org Chem 71:2881–2884
13. Xiang Y, Tong A, Jin P, Ju Y (2006) New fluorescent rhodamine hydrazone chemosensor for Cu(II) with high selectivity and sensitivity. Org Lett 8:2863–2866
14. Yang H, Liu Z, Zhou Z, Shi E, Li F, Du Y, Yi T, Huang C (2006) Highly selective ratiometric fluorescent sensor for Cu(II) with two urea groups. Tetrahedron Lett 47:2911–2914
15. Martinez R, Zapata F, Caballero A, Espinosa A, Tarraga A, Molina P (2006) Rhodamine-diacetic acid conjugate 2-aza-1, 3-butadiene derivatives featuring an anthracene or pyrene unit: highly selective colorimetric and fluorescent signaling of Cu2+ cation. Org Lett 8:3235–3238

16. Zhang X, Shiraishi Y, Hirai T (2007) Cu(II)-selective green fluorescence of a rhodamine-diacetic acid conjugate. Org Lett 9:5039–5042
17. Li G, Xu Z, Chen C, Huang Z (2008) A highly efficient and selective turn-on fluorescent sensor for Cu^{2+} ion based on calix[4] arene bearing four iminoquinoline subunits on the upper rim. Chem Comm 1774–1776
18. Wu S, Liu S (2009) A new water-soluble fluorescent Cu(II) chemosensor based on tetrapeptide histidyl-glycyl-glycyl-glycine (HGGG). Sens Actuators B 141:187–191
19. Ballesteros E, Moreno D, Gomez T, Rodriguez T, Rojo J, Garcia-Valverde M, Torroba T (2009) A new selective chromogenic and turn-on fluorogenic probe for copper(II) in water-acetonitrile 1:1 solution. Org Lett 11:1269–1272
20. Jung HS, Kwon PS, Lee JW, Kim J, Hong CS, Kim JW, Yan S, Lee JY, Lee JW, Joo T, Kim S (2009) Coumarin-derived Cu^{2+}-selective fluorescence sensor:synthesis, mechanisms, and applications in living cells. J Am Chem Soc 131:2008–2012
21. Zhou Y, Wang F, Kim Y, Kim S, Yoon J (2009) Cu^{2+}-selective ratiometric and "off-on" sensor based on the rhodamine derivative bearing pyrene group. Org Lett 11:4442–4445
22. He G, Zhao X, Zhang X, Fan H, Wu S, Li H, He C, Duan C (2010) A turn-on PET fluorescence sensor for imaging Cu^{2+} in living cells. New J Chem 34:1055–1058
23. Goswami S, Sen D, Das NK (2010) A new highly selective, ratiometric and colorimetric fluorescence sensor for Cu^{2+} with a remarkable red shift in absorption and emission spectra based on internal charge transfer. Org Lett 12:856–859
24. Bukowski MR, Zhu S, Koehntop KD, Brennessel WW, Que LJ (2004) Characterization of an Fe^{III}-OOH species and its decomposition product in a bleomycin model system. J Biol Inorg Chem 9:39–48
25. Senthilvelan A, Ho I, Chang K, Lee G, Liu Y, Chung W (2009) Cooperative recognition of a copper cation and anion by a calix[4] arene substituted at the lower rim by a β-Amino-α, β-unsaturated ketone. Chem Eur J 15:6152–6160
26. Benesi HA, Hildebrand JH (1949) A spectrophotometric investigation of the interaction of iodine with aromatic hydrocarbons. J Am Chem Soc 71:2703–2707
27. Singh RB, Mahanta S, Guchhait N (2010) Spectral modulation of charge transfer fluorescence probe encapsulated inside aqueous and non-aqueous β-cyclodextrin nanocavities. J Mol Struct 963:92–97